Vascularization of hepatic structures in a microfluidic platform

Diogo Miguel de Vasconcelos Resende Marques

Instituto Superior Técnico, Lisboa, Portugal

16th of November of 2021

Abstract

Liver disease is a global public health issue that affects from 4.5% to up to 9.5% people worldwide. The only current effective therapy for liver disease is liver transplant - however, the demand for organ donors far exceeds their supply. Thus, a pressing need arises for accurate liver models that allow for better understanding of liver behaviour in health and disease. The present work lays the foundation for the development of vascularized liver organoid and liver tumouroid models by creating a microfluidic culture system in which human umbilical vein endothelial cells (hUVECs) and human mesenchymal stromal cells (hMSCs) are co-cultured with liver organoids or liver tumouroids in a three-dimensional microfluidic environment, supported by a fibrin hydrogel based on pig liver extracellular matrix (ECM). Co-culture of hUVECs and hMSCs in the absence of liver structures led to *de novo* formation of a microvascular network inside the microfluidic device. Angiogenesis was found to be caused by a combination of adequate cell conditioning and culture architecture, as well as by action of the ECM-based hydrogel. Improvements in experimental design are likely to allow for fruitful angiogenic assays in the presence of liver organoids or tumouroids. Furthermore, future applications of this technology include spheroid vascularization, high-throughput screening assays, *in vivo* modelling of human liver and therapeutic approaches.

Keywords: Liver model, liver organoids, ECM hydrogel, microfluidics, vascularization, 3D culture

1. Introduction

According to the World Gastroenterology Organisation (WGO), over fifty million adults are estimated to suffer from chronic liver disease worldwide [1], while liver cirrhosis affects from 4.5% to up to 9.5% of the general global population [2, 3] and hepatocellular carcinoma (HCC) affected over half a million people per year in 2015, with a 5 year survival rate of 10% [1]. In 2015, cirrhosis accounted for 1.16 million deaths and liver cancer accounted for 788,000 deaths, meaning that liver disease-related deaths represented at least 3.5% of all deaths worldwide. However, these numbers are expected to be and underestimation, since they do not account for deaths resulting from acute hepatitis nor from alcohol-use disorders and liver disease is often only diagnosed post-mortem. Furthermore, the number of deaths related to liver disease is expected to rise in the near future, due to the increased frequency in a number of risk factors, such as alcohol consumption, infection with hepatitis B or C (HBV and HCV, respectively), diabetes, obesity and drug consumption [4]. The socioeconomical burden of liver disease is also very heavy. In the U.S. alone, $38 billion were spent in the treatment of liver disease in 2015 [5], while in South Korea yearly investments as high as KRW 8 104 billion (roughly $6.847 billion) were made in therapies against liver disease between 2004 and 2008 [6]. Additionally, liver disease patients in the U.S. have been shown to have a higher probability of being unemployed, having more and heavier disabilities, spending more money on healthcare globally and having a generally lower quality of life than their healthy counterparts [7].

Liver disease cannot be fought without the development of models that provide an accurate depiction of the pathology. However, current animal- or cell-based models have fatal shortcomings that hinder an accurate portrayal of liver behaviour. Animal models, despite useful, are morphologically and immunologically too different from human organisms to be held as adequate [8,9]. Current cell-based models, on the other hand, provide a short-sighted view on disease mechanisms, since they are based on a two-dimensional cellular architecture [10]. They are lacking both three-dimensional cell-cell contact and cell-matrix contact, which are crucial for the proper emulation of *in vivo* cell behaviour [11]. Furthermore, none of these models

have a direct avenue for the delivery of nutrients, mediums or drugs, as would be the case in an *in vivo*, vascularized system. A new approach to *in vitro* liver modeling in the form of liver-on-a-chip devices is rising in popularity, where cells are cultured in a microfluidic system that simulates blood flow [12]. These systems are especially handy in modeling barrier phenomena, such as the uptake of drugs or other molecules. Another route that is currently being pursued is that of liver organoids, small, three-dimensional structures that recapitulate the behavior of a liver [13]. These, when vascularized and immersed in the accurate environment, can provide a model for accurate delivery and metabolization of compounds in the liver. Organoid models of various types have already been developed from human and mouse tissues to treat a multitude of liver diseases, including monogeneic diseases and HCC [14–16].

Having understood the importance of extracellular matrix in the culture of cells, hydrogels are being developed to parallelly improve culture systems by providing an adequate matrix that can not only support the cells, but can actively interact with them, manifesting the necessary cues for their growth and normal behaviour. In this regard, they are often primed to simulate the extracellular matrix of the organ they are meant to replicate [17]. For this purpose, their biological and physicochemical properties, of which porosity, stiffness and degree of cross-linking are particularly noteworthy, are finely tweaked until the best possible balance is achieved [18]. So far, hydrogels for the culture of liver tissues have shown encouraging results, effectively providing support for the growth of hepatic structures [17]. Similarly, the technology of microfluidics has seen staggering growth in the last decade, due to its minimalist approach to cell culture. In microfluidics, the issues of variability and inaccuracy in organ modeling are approached through scaling down the culture system, potentiating surface forces and phenomena and downplaying volume-related forces [19]. This leads to a more controlled and adjustable culture environment, in which the best conditions for cell growth can be provided with consistency [20].

The present work aims at laying the foundation for the fabrication of vascularized healthy liver and liver tumour models by combining organoids, angiogenic cells, and hydrogels into one microfluidic culture system with dynamic medium perfusion. Based on previous works carried out in the lab, where a custom microfluidic device was designed, and a hydrogel that emulates liver extracellular matrix was formulated, this work will attempt to generate vascularized liver tissue in a culture setup that replicates the microenvironment of the liver.

2. Methodology

2.1. Production of dECM-based fibrinogen hydrogel

dECM-based fibrinogen hydrogels are made by mixing 3 base solutions (dECM solution, thrombin solution and fibrinogen solution) in equal proportions. These solutions have their unique composition, as listed below:

- dECM solution (in sterile H_2O Milli-Q®):
  - hyaluronic acid (HA) at 6 $\mathrm{mg\,mL^{-1}}$;
  - dECM powder at 6 $\mathrm{mg\,mL^{-1}}$ from liver matrix decellularized via perfusion with detergent (note: the concentration must be corrected according to BCA results);
  - MEM10X at 20%;
- fibrinogen solution (in sterile H_2O Milli-Q®):
  - fibrinogen at 17.25 $\mathrm{mg\,mL^{-1}}$;
- thrombin solution (in sterile H_2O Milli-Q®):
  - calcium chloride (CaCl2) at 120mM;
  - tranexamic acid (TXA) at $480\,\mathrm{\mu g\,mL^{-1}}$;
  - thrombin at 6.6 $\mathrm{U mL^{-1}}$;
  - MEM10X at 10%.

The three solutions were initially prepared separate from each other in 3 different 1.5ml Eppendorf tubes, or similar. Working concentrations for each solution are three times as high as their concentration in the final hydrogel. The required amount of each reagent is determined by the necessary volume for each solution, which in turn depends on the desired amount of hydrogel.

Thrombin and dECM solutions were each mixed in their own tube and kept in ice. They were pH-corrected to basal medium values (indicated by a light pink colour) with NaOH and HCl solutions, and mixed together. The fibrinogen solution was made at room temperature and kept at 37℃ to avoid precipitation, and swiftly mixed with the combination of dECM- and thrombin solutions via up-and-down pipetting only before applying the hydrogel onto the desired surface. In the case that there are multiple surfaces to be coated with the hydrogel, the tube with the hydrogel solution must remain in ice throughout the charging process. The hydrogel was left to polymerize for 1 hour at 37℃.

2.2. Static 3D co-culture of HepG2, hUVECs and hMSCs

2.2.1 Experimental design

2 conditions were considered, as well as one control, with cell quantity and proportions varied according to table 1. Conditions, as well as the control, were duplicated.

Table 1: Experimental conditions for static co-culture of HepG2, hUVECs and hMSCs.

	Condition 1	Condition 2	Control 1
HepG2	12.500 cells	5.000 cells	No cells
hUVEC	10.000 cells	4.000 cells	8.000 cells
hMSC	2.500 cells	1.000 cells	2.000 cells
TOTAL	25.000 cells	10.000 cells	10.000 cells

The experiment was performed on a flat-bottom 24-well plate, with 2 wells per condition, which were filled with angiogenic medium, and the remainder of the wells were filled with H_2O MilliQ. Medium was changed when deemed necessary, or at least once every 3 days.

2.2.2 Angiogenic medium preparation

Medium was prepared according to the formulation seen in Table 2. Volumes too small to pipette were diluted, and the volume of MCDB 131 was adjusted accordingly.

Table 2: Formula for the preparation of $30\mathrm{mL}$ of angiogenic medium.

Medium component	*Volume*
DMEM F12	13.937mL
MCDB 131	13.937mL
L-glut (1%)	300uL
PS (1%)	300uL
FBS (5%)	1.5mL
Insulin (10mg/mL → 50ng/mL)	15uL
Transferrin (50mg/mL → 10ug/uL)	6uL
VEGF (1mg/mL → 50 ng/mL)	1.5 uL
EGF (1mg/mL → 20 ng/mL)	0.6uL (actually1.2uL)
FGF (1mg/mL → 20 ng/mL)	0.6uL (actually1.2uL)
IGF-1 (1mg/mL → 20 ng/mL)	0.6uL (actually1.2uL)

2.2.3 Preparation of dECM-based fibrinogen hydrogel droplets

Hydrogel was prepared as discussed in subsection 2.1 for a total volume of $600\mu\mathrm{L}$. Cell were harvested and incorporated into the hydrogel by scraping and up-and-down pipetting of their dry pellets with the mixture of pH-corrected dECM and thrombin solutions in each tube, creating a homogeneous cell-in-hydrogel suspension. The tubes were put in ice and the fibrinogen solution was then added to each individual Eppendorf tube. Duplicates were made by taking two droplets of $50\ \mu\mathrm{L}$ each from each Eppendorf tube and placing them gently in a flat-bottom 24-well plate. The plate was incubated at 37℃ for 1 hour before medium was added.

2.3. mRNA characterization of tumouroids, organoids, hUVECs, HepG2 cells and native liver

mRNA characterization of organoids (generated by conditioning of isolated EpCAM-positive cells) and tumouroids (generated by hanging-drop culture of HepG2 cells) was obtained via RT-PCR of lysed tumouroids and organoids. Harvested structures were placed in $100\ \mu\mathrm{L}$ or $300\ \mu\mathrm{L}$ TRIzol™reagent (depending on sample size) and stored at -30℃ until they were needed for mRNA isolation.

For mRNA isolation, samples were thawed out, diluted in chloroform, and genetic material was precipitated in isopropanol. Results for RNA purity and quantity were measured by a NanoDrop microvolume spectrometer. cDNA was created from the mRNA sample by incubating reverse transcriptase.

Primers for human VEGF, HiF1-α, HGF, Ki-67, ITGB1, ITGB3, NOS3, ETV2, COX-2, KLF2 and RAP1 genes were determined with ncbi's primer designing tool. Verified primers for GAPDH, albumin genes already existed in the lab. Polymerase chain reactions (PCRs) were then carried out in temperatures from 54℃ to 64℃ with a two-degree step increase to assess the optimal working temperatures of each primer, while simultaneously verifying the amplification of mRNA for each gene, for each sample.

2.4. Dynamic cell culture in bioreactor

2.4.1 Bioreactor setup

The bioreactor consisted of circuits of silicone tubes connected to the microfluidic device which were driven by a Hei-FLOW Precision 01 peristaltic pump lent to us by José Manuel García Aznar's lab at the I3A. Each chip, which was designed in-house and previously made by molding on a silica wafer, was connected to two circuits: artery (top) and vein (bottom). Silicon tubes by MaterFlex® (with an inner diameter of $1.4\mathrm{mm}$) were attached to each other with proper fittings and four-way stopcocks. $20\ \mathrm{mL}$ syringes were used as medium reservoirs (one for each circuit), where the piston was set at roughly $10\ \mathrm{mL}$.

2.4.2 Culture conditions

Cells were cultivated at 37℃, in normoxia. Culture medium used depended on the presence or absence of liver structures. Flow was set at $2\mathrm{mL\,min^{-1}}$, but was turned off for as long as 48h when empirically deemed necessary, in order to cause starvation. Medium changes occurred at most every 5 days, or whenever necessary.

2.4.3 Liver-free angiogenic assay

For this experiment, 300k cells were prepared per microfluidic chip, of which 80% (240k) were hUVECs and 20% (60k) were hMSC. Upon preparation of the dry cell pellet, cells were suspended in $120\ \mu\mathrm{L}$ of dECM hydrogel or $120\ \mu\mathrm{L}$ of Matrigel®

, and loaded into the central chamber of 2 different chips 60 μL of cells suspended in Matrigel went into the central chamber of chip 1 (with 15 μL being pipetted every time), while the central chamber of chip 2 was filled with the same amount of cells suspended in fibrinogen-based hydrogel. The remaining 60 μL of each hydrogel were distributed along the vessels of their respective chips via the superior and inferior charging ports. Custom dECM hydrogel was used for all following liver-free angiogenic assays. A previously cut small, ring-like segment of blood vessel was inserted through the central port of each chip. This process must be performed swiftly, to avoid untimely gel polymerization, yet carefully, to avoid air bubbles. The system was left to polymerize for 1 hour before it was incorporated into a bioreactor with angiogenic medium. The dynamic culture system was maintained for up to two weeks, and imaged daily. Medium was changed whenever leaks caused the medium reservoirs to be depleted, or once every 4 days. Chips that showed promising structures were fixed by perfusion with PFA 4% through both artery and vein perfusion channels for 15 minutes, and stored at room temperature.

2.4.4 Tumouroid and Organoid angiogenic assays

Here, the same protocol was applied as in section 2.4.3. However, for the case of tumouroids, those of sizes ranging from 5k cells to 20k cells were pelleted and resuspended in the hydrogel alongside hUVECs and hMSCs. Different experiments were carried out to determine the best type and amount of tumouroids to introduce in the hydrogel, which are further detailed in the complete dissertation. Organoids were pelleted and resuspended into the hydrogel alongside other cells, and introduced into the central chamber. For organoid-based angiogenic assays, a hybrid organoid and angiogenic medium was used (Table 3). All tumouroid- and organoid-related assays were performed with dECM-based fibrin hydrogel, and none with Matrigel® .

2.4.5 Imaging

Day-to-day pictures of cell cultures, both in static and dynamic conditions, were obtained with NIS Elements 3.0 software in combination with the Nikon DS-Fi1 camera attached to the Nikon Eclipse TS100 microscope. For the fluorescence time-lapse imaging, the setting of of a bioreactor was emulated, where fluorescein isothiocyanate–dextran (FITC-Dextran) was dissolved into the medium at a concentration of 25 $\mathrm{mg\,mL^{-1}}$, and perfused at 0.6

Table 3: Composition of hybrid angiogenic/organoid medium for dynamic angiogenic assays with liver organoids. GLX, P/S, EGF and FGF concentrations were omitted from one medium composition to avoid redundancy when the medium component was present in both the angiogenic and organoid-related aspects of the medium.

Angiogenic component		Organoid component	
MCDB 131	(50% of leftover volume)	Advanced DMEM/F12	(50% of leftover volume)
GLX	2%	GLX	---
P/S	---	P/S	1x
FBS	2%	HEPES	10mM
Insulin	5 µg/ml	B27 (+ins/-vit A)	1x
Transferrin	10 µg/ml	N2	1x
VEGF	50 ng/ml	NIC	10mM
EGF	---	ROCK inhibitor	10 µM
FGF	---	R-spondin 1	10%
IGF-1	20 ng/ml	NAC	1.25mM
		A8301	5 µM
		Forskolin	10 µM
		FGF10	100ng/ml
		EGF	50 ng/ml
		HGF	25 ng/ml
		Gastrin	10nM

3. Results

3.1. Generation of liver decellularized extracellular matrix hydrogel

The decellularization was performed as shown in Figure 1. Decellularized liver samples were divided into 1^{st}- and 2^{nd}-grade, according to their apparent degree of decellularization. Decellularization rates as measured by DNA quantification with NanoDrop-assisted spectrophotometry were of over 97% for first-grade liver and over 81% for second-grade liver, with a total sample quantity of 24.67 g and 23.68 g, respectively, and samples showed an adequate degree of purity. Protein concentration in decellularized ECM was calculated with a bicinchoninic acid (BCA) assay, which revealed a correlation factor of 0.3015 g of protein per every gram of dECM powder.

The hydrogel itself was made by combining the dECM with water-based thrombin and fibrinogen solutions in a 1:3 ratio. Next, the mix is plated onto a 24-well plate well and left to polymerize for 1 hour. During polymerization, the thrombin molecules cleave the fibrinogen chains into fibrin molecules, which quickly connect to form a polymeric network, encapsulating the proteins from the decellularized liver matrix.

We have found this hydrogel to be capable of forming cohesive, self containing drops in which cells can proliferate, both in a macroscopic setting and in a microfluidic system. Furthermore, decellularization results obtained here are on par with those seen in literature, solidifying this hydrogel as an emulator for liver extracellular matrix [21, 22].

3.2. Static 3D co-culture of hUVECs, hMSCs and HepG2 cells

Before any cells were cultured in the hydrogel, its formulation was adjusted by performing a trial in which thrombin concentrations were increased in

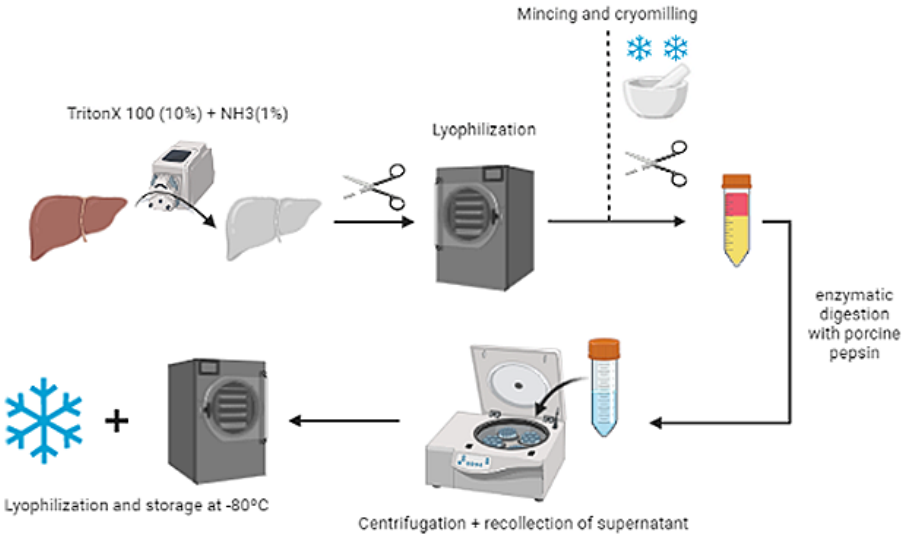

Figure 1: Overview of liver ECM processing workflow. After liver decellularization, adequate samples are sectioned and lyophilized Lyophilization results are then mechanically processed by mincing and cryomilling before undergoing enzymatic digestion cycles with porcine pepsin. Supernatants are collected and centrifuged, after which they are once more lyophilized. Created with BioRender.com.

steps of 0.025 $\mathrm{U mL^{-1}}$, ranging from 2.1 $\mathrm{U mL^{-1}}$ to 2.5 $\mathrm{U mL^{-1}}$. Optimal thrombin concentration was found to be 2.2 $\mathrm{U mL^{-1}}$, with this result being applied in all hydrogel cultures of this work.

A static co-culture of human umbilical vein endothelial cells (hUVECs), human mesenchymal stromal/stem cells (hMSCs) and HepG2 cells was then set up in a macrofluidic 50 µL drops of liver dECM hydrogel, to provide a stepping stone towards the microfluidic implementation of the protocol. Given their tumorigenic phenotype, HepG2 cells were expected to secrete angiogenic factors that would aid in the organization of hUVECs into small blood vessels, with the latter possibly exhibiting tropotrophic behaviour in relation to the former. Upon seeding, cells seemed homogeneously distributed throughout the drop, with very few clumps or aggregates. The drops polymerized in a cohesive manner, without apparent cracks or flaws. Organization of some type can be seen after four days of culture, but not in a significant manner. Additionally, hydrogel drops degraded over time, which caused the cells to latch on to the bottom of the plate, defeating the purpose of a 3D culture - which led to an early stop of this experiment.

These results were rather surprising, since the liver dECM hydrogel should provide all the necessary conditions for the growth of microvascular structures. However, various caveats of the experiment, like the short culture period, the degradation of the drops, and the utilization of cells in numbers and proportions that had previously not been tested. Nevertheless, it was not worthwhile to invest any further into this experiment, since the goal of the present work is tied with the incorporation of microfluidics.

3.3. Static expansion of liver organoids and liver tumouroids

Liver organoids and liver tumouroids to be introduced in dynamic, microfluidic culture were previously expanded in static conditions. Tumouroids were formed via the hanging-drop method, where 5k, 10k, 15k or 20k HepG2 cells were suspended in drops of 30 µL of culture medium, and cultured upside-down to form aggregates. Organoids were expanded in 24-well plates on a Matrigel® substrate and immersed in conditioning medium.

It was found that the hanging drop method was effective in forming 3D HepG2 aggregates at all concentrations after only 5 days of hanging-drop culture. Figures 2 a) to d) show the results of static tumouroid assembly cultures, where tumouroid size increases from 5k cells/drop tumouroids to 10k cells/drop tumouroids, but no significant changed are detected between 10k cells/drop tumouroids and 15k- or 20k cells/drop tumouroids. Importantly, however, well-defined tumouroids were formed in all cases.

Organoid formation was also successful, as can be seen in Figures 2 e) and f). Hepatic organoids formed this way were clear and self-containing. Importantly, organoid expansion seems to have resulted in a high number of valid hepatic organoids, which will be later incorporated into a microfluidic bioreactor.

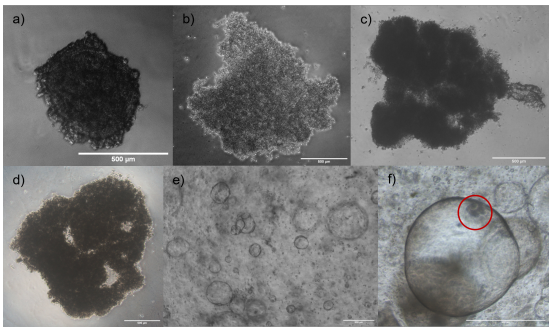

Figure 2: a)-d) Static, three-dimensional culture of HepG2-based liver tumouroids with 5k, 10k, 15k and 20k cells per 30 ul drop, respectively. Structures seem cohesive, with size discrepancies between 5k cell-structures and bigger tumouroids. e) Static, three-dimensional culture of hepatic organoids with apparent good proliferation and structure (4x). f) Close-up on static organoid culture, highlighting an internal structure of the organoid (10x). Scale bars = 500 μm

Table 4: Characterization of mRNA expression of different genes (left column) in samples (top column), as detected by polymerase chain reaction and gel electrophoresis. NT = Not Tested.

	hUVECs	Organoids	Tum1	Tum2	HepG2	Native Liver
ITGB1	Yes	NT	NT	NT	NT	Yes
ITGB3	Yes	NT	NT	NT	NT	Yes
NOS3	Yes	NT	NT	NT	NT	Yes
COX2	No	NT	NT	NT	NT	No
ETV2	No	NT	NT	NT	NT	No
KLF2	No	NT	NT	NT	NT	No
RAP1	Yes	NT	NT	NT	NT	Yes
HiF1-α	NT	Yes	Yes	No	Yes	Yes
HGF	NT	No	No	No	No	Yes
Ki-67	NT	No	No	No	No	No
GAPDH	Yes	Yes	Yes	Yes	Yes	Yes
VEGF	NT	No	No	No	Yes	No
ALB	NT	Yes	No	Yes	Yes	Yes

3.3.1 Characterization of liver organoid and tumouroid mRNA expression

mRNA characterization of tumouroids and organoids yielded the results shown in Table 4. From those tested, hUVEC culture expressed angiogenic genes typical of healthy liver and did not show expression of tumour-related angiogenic genes nor of those related to the inhibition of angiogenic pathways. Simultaneously, 3D liver-like structures emulated mRNA expression of the liver in all tested genes, except for HGF. Interestingly, the tumouroid samples that were analysed showed differential expression amongst themselves, exclusively expressing HiF1-1α or ALB, which are characteristic markers of liver function. Differential expression was also seen between tumouroids and HepG2 cells, with the latter, but not the former, expressing VEGF. Lastly, Ki-67 was ubiquitously absent, while GAPDH, which served as a loading control, was ubiquitously expressed.

3.4. Liver-free angiogenic assays

Liver-free angiogenic assays consisted of the co-culture of hUVECs and hMSCs supported either with Matrigel® or dECM hydrogel in our microfluidic, dynamically perfused device.

Cultures supported by Matrigel® found no success in what regards *de novo* vessel formation, whereas two out of three trials with dECM-based fibrin hydrogel cultures succeeded in the formation of microvascular networks. Blood vessels formed this way were well-defined, and branched to connect to each other.

These are major results, since they prove that *de novo* angiogenesis is possible with our microfluidic system, meaning that the possibility of vascularized liver models is well within sight. Furthermore, angiogenesis occurred in more than one trial, attesting to the reproducibility of the system and the robustness of the results. Notably, vessel formation did not occur on the same culture day in both cases, with fist signs of tube formation showing on day 1 or day 5.

3.5. Organoid and tumouroid angiogenic assays

Lastly, we attempted to generate an equally vascularized network in systems which contained liver structures. Although some signs of possible vascularization can be seen, there was no trial that showed as much success as those performed in systems without tumouroids and organoids. While tumouroid trials lacked in consistency, since the protocol was being optimized on a trial-and-error basis, the only organoid trial that was carried out showed inconclusive results due to experimental failure.

4. Discussion

Results seen here, despite presenting a varying degree of significance in the context of the work, are all crucial building blocks for the development of a microfluidic-based, 3D vascularized liver model.

The generation of liver dECM hydrogel was successful, as it resulted in cohesive drops which polymerized at an adequate temperature, and contained liver ECM proteins. Furthermore, the hydrogel proved to be an adequate environment for the culture of cells, and was reliably reproduced. Unlike Matrigel® , our dECM-based fibrin hydrogel is specific to the liver and can easily be adapted to be xenogeneic-free, by replacing porcine liver matrix with human liver matrix. This feat opens the door to more accurate modeling of the human liver or even to the upscaling of these models with the goal of introducing them in clinical practice [23].

Liver tumouroid and organoid formation and expansion yielded satisfactory results, since robust structures with adequate morphology were formed in both cases. However, size differences in HepG2 tumouroids are particularly remarkable, since they are mostly seen from tumouroids with 5k cells

to those with 10k cells. Tumouroids with higher amounts of cells condensed onto themselves, possibly to avoid a necrotic cell core [24]. mRNA expression analysis of tumouroids and organoids showed that there is differential expression between both types of structures, but also between each one of them and the liver. The absence of expression of HGF in liver spheroids is especially important, since it might denote that structures are still immature. Nevertheless, the presence of liver-specific mRNA in tumouroid and organoid samples indicates their viability as liver models, while the confirmed expression of angiogenesis-related genes by hUVECs further solidifies their capabilities in the formation of blood vessels. Thus, it quickly becomes evident that a co-culture of hUVECs and liver organoids or tumouroids is an important stepping stone for the development of a vascularized liver model. In future experiments, it might be of great interest to characterize mRNA expression of the microfluidic system and compare it with the results obtained here, so as to infer the true impact, as well as the real potential of a dynamic, microfluidic co-culture of liver structures and angiogenic cells.

The most important result of this work is unarguably the generation of microvascular networks in the central chamber of the microfluidic device. Here, the angiogenic role of the dECM hydrogel was also shown, as all conditions where a vascular network was generated incorporated the fibrin-based hydrogel. While the vascularization of tumouroid and organoid structures was not as successful, we hypothesize that protocol modifications, both in the experimental design and in the generation of the hydrogel, will allow for an improvement in results. Thus, it is expected that the same basic methods used here will be able to produce vascularized models of healthy or cancerous liver. As far as we are aware, it is the first time that angiogenesis was achieved in a perfused system with a liver dECM hydrogel.

4.1. Future perspectives

[redacted]

5. Conclusions

Liver disease is a public health problem responsible for over 3.5% (2 million) of all deaths per year, worldwide [4], with patients affected by liver disease being affected by other comorbidities. The development of novel therapies hinges on the deep understanding of the liver and its mechanisms, which themselves depend on the existence of accurate models of healthy and damaged liver behaviour. In this work, we lay the foundation for the production of a vascularized, three-dimensional model for healthy and cancerous liver in a microfluidic setting.

This thesis based itself on the current state-of-the-art in hydrogel-, microfluidics- and organoid applications, as well as on previous research conducted in our lab, to successfully stimulate *de novo* angiogenesis in a three-dimensional microfluidic culture supported by a dECM-based hydrogel. To do so, hUVECs and hMSCs grown in two-dimensional cultures were incorporated in a bioreactor setup with continuous flow driven by a peristaltic pump, where they were cultured with angiogenic medium and formed an interconnected microvascular network in two out of three trials. Besides constituting the foundation for further work, this result validates the dECM-based hydrogel and the microfluidic chip used in the bioreactor system, which were both developed in our lab.

These principles were then applied to try and generate a culture of vascularized liver organoids and tumouroids. Characterization of mRNA expression showed that organoids and tumouroids expressed some, but not all of the markers seen in native liver. These hepatic spheroids, which had previously been expanded in 3D culture, were incorporated into the microfluidic platform alongside hUVECs and hMSCs. In all five performed trials (four with tumouroid cultures and one with an organoid culture), it was not possible to see signs of robust angiogenesis, unlike what happened in liver-free cultures. However, it is expected that more repetitions of these experiments with adequate optimizations yield positive results, even more so taking into account previous results from our group.

In this work, a proof of concept was successfully carried out in that a microvascular network was created, leaving the task of the adaptation into cultures with organoids and tumouroids for a further study. The technology developed in this project can be used to lay the foundation for the development of a model for healthy and cancerous human liver, which can in turn be used in a number of biomedical applications. If these prove to be successful, the technology used in this work can be modified to be used in other spheroid-capable tissues, such as kidney and pancreas.

References

[1] S. K. Sarin and R. Maiwall. Global burden of liver disease: A true burden on health, sciences and economies.

[2] M. Melato, F. Sasso, and F. Zanconati. Liver cirrhosis and liver cancer. a study of their relationship in 2563 autopsies. *Zentralbl Pathol.*, 139(1):25–30, 1993.

[3] YS. Lim and WR. Kim. The global impact of hepatic fibrosis and end-stage liver disease. *Clin Liver Dis.*, 12(4):733–46, 2008.

[4] S.K. Asrani, H. Devarbhavi, J. Eaton, and P.S. Kamath. Burden of liver diseases in the world. *J Hepatol.*, 70(1):151–171, 2019.

[5] A.F. Peery, S.D. Crockett, C.C. Murphy, J.L. Lund, E.S. Dellon, J.L. Williams, E.T. Jensen, N.J. Shaheen, A.S. Barritt, S.R. Lieber, B. Kochar, E.L. Barnes, Y.C. Fan, V. Pate, J. Galanko, T.H. Baron, and R.S. Sandler. Burden and cost of gastrointestinal, liver, and pancreatic diseases in the united states: Update 2018. *Gastroenterology*, 156(1):254–272, 2019.

[6] Sunmi Lee, Woojin Chung, and Kyung-Rae Hyun. Socioeconomic costs of liver disease in korea. *The Korean journal of hepatology*, 17(4):274, 2011.

[7] Maria Stepanova, Leyla De Avila, Mariam Afendy, Issah Younossi, Huong Pham, Rebecca Cable, and Zobair M Younossi. Direct and indirect economic burden of chronic liver disease in the united states. *Clinical Gastroenterology and Hepatology*, 15(5):759–766, 2017.

[8] Michela Anna Polidoro, Erika Ferrari, Simona Marzorati, Ana Lleo, and Marco Rasponi. Experimental liver models: From cell culture techniques to microfluidic organs-on-chip. *Liver International*, 41(8):1744–1761, 2021.

[9] Yan Liu, Christoph Meyer, Chengfu Xu, Honglei Weng, Claus Hellerbrand, Peter ten Dijke, and Steven Dooley. Animal models of chronic liver diseases. *American Journal of Physiology-Gastrointestinal and Liver Physiology*, 304(5):G449–G468, 2013.

[10] Patricio Godoy, Nicola J Hewitt, Ute Albrecht, Melvin E Andersen, Nariman Ansari, Sudin Bhattacharya, Johannes Georg Bode, Jennifer Bolleyn, Christoph Borner, Jan Boettger, et al. Recent advances in 2d and 3d in vitro systems using primary hepatocytes, alternative hepatocyte sources and non-parenchymal liver cells and their use in investigating mechanisms of hepatotoxicity, cell signaling and adme. *Archives of toxicology*, 87(8):1315–1530, 2013.

[11] Sarah M Maritan, Eric Y Lian, and Lois M Mulligan. An efficient and flexible cell aggregation method for 3d spheroid production. *Journal of visualized experiments: JoVE*, (121), 2017.

[12] Fuyin Zheng, Fanfan Fu, Yao Cheng, Chunyan Wang, Yuanjin Zhao, and Zhongze Gu. Organ-on-a-chip systems: microengineering to biomimic living systems. *Small*, 12(17):2253–2282, 2016.

[13] Christopher J Hindley, Lucía Cordero-Espinoza, and Meritxell Huch. Organoids from adult liver and pancreas: stem cell biology and biomedical utility. *Developmental biology*, 420(2):251–261, 2016.

[14] Meritxell Huch, Helmuth Gehart, Ruben Van Boxtel, Karien Hamer, Francis Blokzijl, Monique MA Verstegen, Ewa Ellis, Martien Van Wenum, Sabine A Fuchs, Joep de Ligt, et al. Long-term culture of genome-stable bipotent stem cells from adult human liver. *Cell*, 160(1-2):299–312, 2015.

[15] Yuan Guan, Dan Xu, Phillip M Garfin, Ursula Ehmer, Melissa Hurwitz, Greg Enns, Sara Michie, Manhong Wu, Ming Zheng, Toshihiko Nishimura, et al. Human hepatic organoids for the analysis of human genetic diseases. *JCI insight*, 2(17), 2017.

[16] Jarno Drost and Hans Clevers. Organoids in cancer research. *Nature Reviews Cancer*, 18(7):407–418, 2018.

[17] Shicheng Ye, Jochem WB Boeter, Louis C Penning, Bart Spee, and Kerstin Schneeberger. Hydrogels for liver tissue engineering. *Bioengineering*, 6(3):59, 2019.

[18] Wenda Wang, Ravin Narain, and Hongbo Zeng. Hydrogels. In *Polymer Science and Nanotechnology*, pages 203–244. Elsevier, 2020.

[19] Jing Wu and Min Gu. Microfluidic sensing: state of the art fabrication and detection techniques. *Journal of biomedical optics*, 16(8):080901, 2011.

[20] Francesca Bragheri, Rebeca Martínez Vázquez, and Roberto Osellame. Microfluidics. In *Three-Dimensional Microfabrication Using Two-Photon Polymerization*, pages 493–526. Elsevier, 2020.

[21] Pedro M Baptista, Mohummad M Siddiqui, Genevieve Lozier, Sergio R Rodriguez, Anthony Atala, and Shay Soker. The use of whole organ decellularization for the generation of a vascularized liver organoid. *Hepatology*, 53(2):604–617, 2011.

[22] Paul Lin, Warren CW Chan, Stephen F Badylak, and Sangeeta N Bhatia. Assessing

porcine liver-derived biomatrix for hepatic tissue engineering. *Tissue engineering*, 10(7-8):1046–1053, 2004.

[23] Cell culture dish. Xeno-free, what is it?

[24] Eiji Takahashi. Anoxic cell core can promote necrotic cell death in cardiomyocytes at physiological extracellular po2. *American Journal of Physiology-Heart and Circulatory Physiology*, 294(6):H2507–H2515, 2008.